3D printed lab on a chip with microelectronics and silicon integration

D.J. Thomas [a], C.A. McCall [b] and Z. Tehrani [b]
[a] Yale School of Engineering and Applied Science, 10 Hillhouse Ave, New Haven
[b] Swansea University, College of Engineering, Bay Campus, Swansea

Abstract
In this research an integrated 3D printed laboratory on a chip system was developed based on integrating conventional silicon bio-sensing systems with silver screen printed electronics. It was found that by integrating 220µm width micro-channels, fabricated using 3D printed polymers, that this offered a means for the development of a microfluidic device with the further possibility for electrically integrating different elements through depositing screen-printed silver contacts. The objective was to achieve low resistance and high reliability with low cost for manufacturing 3D printed point of care (POC) diagnostic devices.
Keywords: Microfluidics, Lab on a chip, Point of Care Systems, 3D Printing.

1. Introduction

Integrating printed electronics with silicon nanowire sensor technology can be used to fabricate microfluidic-based sensing platforms. Microfluidic-based MEMS handle fluid flow in the µL quantity, however, there is a limited use of these devices as commercial systems. Various applications of MEMS in the biomedical field have been reported in such applications as; therapeutic microsystems, surgical microsystems and drug therapy delivery systems. In order to explore the concept of integrating microfluidic elements with a nanowire sensing platforms. Such systems incorporate nanowires with different functionalised biomarkers **[1-5]**. Source and drain electrodes are insulated from the fluid environment by a dielectric passivation layer, and a polymer embedded microfluidic channel enables rapid solution delivery to arrays of nanowiredevices **[6-10]**.

The relative size of nanowire devices, enable thousands of individual addressable nanowires to be housed within a single microfluidic delivery microchannel. Significantly, defining distinct surface receptors on different nanowire elements opens up the potential for multiplexed, real-time assays of multicomponent solutions, such as the simultaneous detection of biomarker proteins, viruses and small molecules. State-of-the-art nanowire sensor arrays fabricated in this way can contain more than a hundred independently addressable nanowire elements. A microfluidic channel mated to the chip can be used as a route toward screening complex biological fluids and would have significant prospects in the detection of disease. A key issue that prevents the commercialisation of fully integrated systems for personalized medicine applications is the disposability of the assay-substrate at a low cost **[11-12]**.

A standard microfluidic platform consists of a combinable set of microfluidic unit-operations that allows analysis miniaturisation within a conventional fabrication

technology. The function of lateral flow strip tests use capillary forces to drive liquids along a microchannel in which movement is controlled by the porous substrate with the agents stored within the test strip. As **[13]** reported, the results are measured by eye, and indicated by a colour change or in the materialisation of a visual area. Each pad within the test strip represents different functions including; loading, reagent pre-storage, reaction, detection, absorption and liquid actuation. The characteristic unit operation of this system is passive liquid transport using capillary forces. The absorption volume of an absorption pad defines how much sample pulled through the strip and provides a precise volume control mechanism **[14]**. As **[15-18]** reported, the conjugates are typically coloured or fluorescent 800nm nanoparticles, which flow without obstruction through together with the sample.

Pressure driven laminar flow systems show good agreement between laboratory results and POC-systems **[17,19]**. Here a pressure gradient is used to transport liquids through the use of internal pressure sources such as pumps or micropumps, gas expansion or pneumatic displacement of membranes. Samples and reagents are processed by injecting them into microchannels which is a process that is laminar over a wide range of flow rates and microchannel dimensions. Pressure driven laminar flow provides the advantages of:

- Predictable velocity profiles;
- Controllable diffusion mixing;
- Stable phase arrangements in co-flowing streams.

It is these key advantages that have been utilised for many several lab-on-a-chip applications. A conventional technology, as developed by Huh et al. (2005), **[20]** used hydrodynamic focusing technology to align cells in continuous flow for analysis. Key technologies use laminar flow effects for particle counting Wu et al. (2008) **[21]**, or separation **[22]**. Pressure driven laminar flow can also be utilised to implement other mechanisms of analysis for lab-on-a-chip applications. For instance, as Woolley et al. (1996) **[23]** reported, nucleic acid-based diagnostic systems have been developed since the first introduction of a combined microfluidic and capillary electrophoresis device. The function of operation on the pressure driven laminar flow platform is the contact of multiple liquid streams at a microfluidic channel junction. This leads to controlled diffusional mixing at the phase interface for initiation of a biological/chemical reaction has been achieved **[24]**.

A variety of valving principles exist on pressure driven laminar flow systems as summarised by **[25]** who presented a review of active as well as passive solutions. A further development is to transfer the valving functionality off-chip as **[26]** demonstrated, which resulted in decreasing the complexity and cost of the disposable POC-system. Here devices have been fabricated to provide liquid actuation and off-chip valving by stopping liquid flow from the exits of the biochip.

2. Research Methods

2.1. 3-D Printing the Microfluidic Device

Fused deposition 3-D printing processes was used to deposit Aliphatic Polyurethane Polymer (APP) and produce a microfluidic-based device. A layer resolution of 100µm was used during the 3D printing process in order to produce micro-channels which had the required level of accuracy to produce a 200µm width microchannel. The parameters used during the 3-D Printing process are shown in **Table 1**.

Table 1. 3D Printing Process Parameters

Printing Parameter	**Value**	**Unit**
Layer Thickness	100	µm
Print Speed	50	mm/s
Number of Shells	5	-
Temperature (extruder)	220	^{o}C
Temperature (build platform)	120	^{o}C
Diameter of extruded plastic	400	µm

2.2. Screen Printed Contacts

A DEK 248 screen printing press under ambient air conditions was used to print silver ink (Henkel) 65% solid content onto the surface of the 3D printed device. The 3D printed device was cleaned using isopropyl alcohol (IPA) before screen printing. The connection lines printed were 200µm in width. Parameters used during the screen printing process are shown in **Table 2**.

Table 2. Process parameters used during the screen printing process.

Parameter	Setting
Forward and reverse speed	70 mm/s
Print gap	2.0 mm
Separation speed	100 %
Pressure	10 kg

Curing of the ink was carried out at 170°C for one hour. These printed contacts were electrically characterised using a four point probe to determine the resistances in each of the contacts printed, in which the contact resistance was 45µΩ-cm.

2.3. Microscopy and Spectroscopy

Screen printed 3D printed devices were electrically characterised to understand the electrical conductance of the ink. White light profiles using a WYKO White Light Interferometer were made with a scan area of 0.92 x 1.2mm to determine the profile of the screen printed contacts produced. Scanning electron microscopy (SEM; Ultra-

High Resolution FE-SEM S-4800, Hitachi) was carried out at 10kV acceleration voltage and a 9.8mA emission current. A magnification of x2200 and the working distance was 29.9mm. The SEM scan resolution was 640x480 pixels.

2.4. Silicon Nanowire Biosensor Fabrication

A four silicon nanowire array was fabricated on (5mmx5mm) $25mm^2$ SOI substrates. The silicon was first cleaned using a solvent, acid and alkali cleaning procedure, followed by a 10 second hydrofluoric acid (HF) immersion. Silicon nanowires were fabricated using electron beam lithography (EBL) (Raith E-Line Instrument, Raith) and photolithography (Mask Aligner, MA/BA8 Gen 3 from SUSS MicroTec). PMMA-coated silicon substrates were spin-coated with PMMA using a spin speed of 4000 rpm for 40 seconds to produce a film thickness of 250nm. The PMMA was soft-baked at 85°C for 2 minutes before exposure to the electron beam for the direct-write EBL process. The Silicon nanowire device consists of two 0.5mm x 0.5mm sized contact pads at either end of a silicon nanowire. Four nanowire lengths on 50µm, 100µm, 300µm and 500µm. The PMMA was patterned using the following EBL parameters:

Aperture size = 30 µm;
Acceleration voltage = 10 kV and
Beam current = 0.201nA.

The contact pads of the device were patterned using an exposure of $100\mu A/cm^2$, and the Silicon nanowire pattern was written using an exposure of $500pAs/cm^2$. The sample was developed in isopropyl alcohol (IPA): methyl isobutyl ketone (MIBK) = 3:1) for 1 minute. A lift-off process, using a 100nm Al coating deposited using a KJ Lesker PVD 75 Sputtering System on top of the nanoscale PMMA pattern, was used to define an Al hard mask on top of the silicon substrate. The Al mask was used to selectively protect areas of silicon during the Reactive Ion Etching process. Following etch removal of the exposed areas of the 200nm silicon layer that were not protected by the Al mask, a single crystalline Silicon nanowire was formed.

A second 1µm thick Al deposition step was then performed and metal contact pads were defined using standard photolithography process (using a SUSS MicroTec MA/BA8 Gen 3 Mask Aligner and AZ ECI3027 positive-tone resist from AZ Materials) with metal etch-back. The sample was then thermally annealed using Rapid Thermal Annealing process gas of 50 sccm nitrogen (N_2) at 400°C for 5 minutes in order to form an ohmic contact.

3. Results and Discussion

3.1. 3D Printed Laboratory on a Chip

The microfluidic point of care device was developed on the concept of integrating screen printed electrical connections with a 3D Printed microfluidic channel within a device. Following the fabrication process, the device was integrated with a silicon nanowire-based sensor. **Figure 1** shows the concept laboratory on a chip design, which integrates the biosensor. The electrical connection is based on a flip-chip contact principle, in which the chip is connected to the screen printed electrical connections facedown.

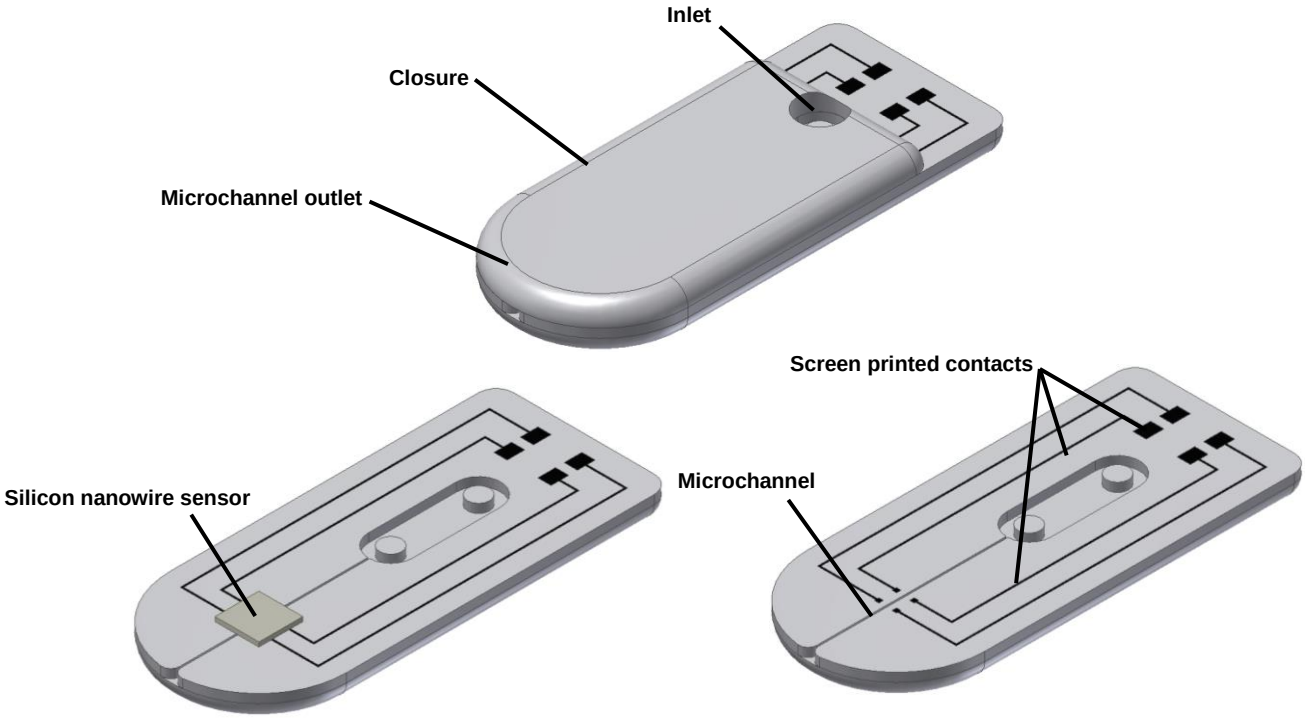

Figure 1. Design of the 3D Printed point of care device with integrated screen printed contacts and silicon nanowire sensor.

The microfluidic device is made up of two 3D Printed polymer components. These have the integration of screen printed contacts which connect to a silicon nanowire biosensor chip. The polymer used to make the point of care device is medical-grade aliphatic polyurethane.

3.2. 3D Printed Microfluidics

As **Figure 2** shows the lab on a chip has a 220µm width 3D Printed microchannel at the centre of the structure. These were produced successfully at a printing speed of 50mm sec $^{-1}$. This set of 3D printing process parameters allowed for the accurate fabrication of microchannels which were 384µm in height. Here, the SiNW which sits over this microchannel are exposed to the fluid flow. By controlling the surface area of the nanowire and the volume of the liquid within the microchannel then the precise quantity of fluid analysed can be accurately controlled.

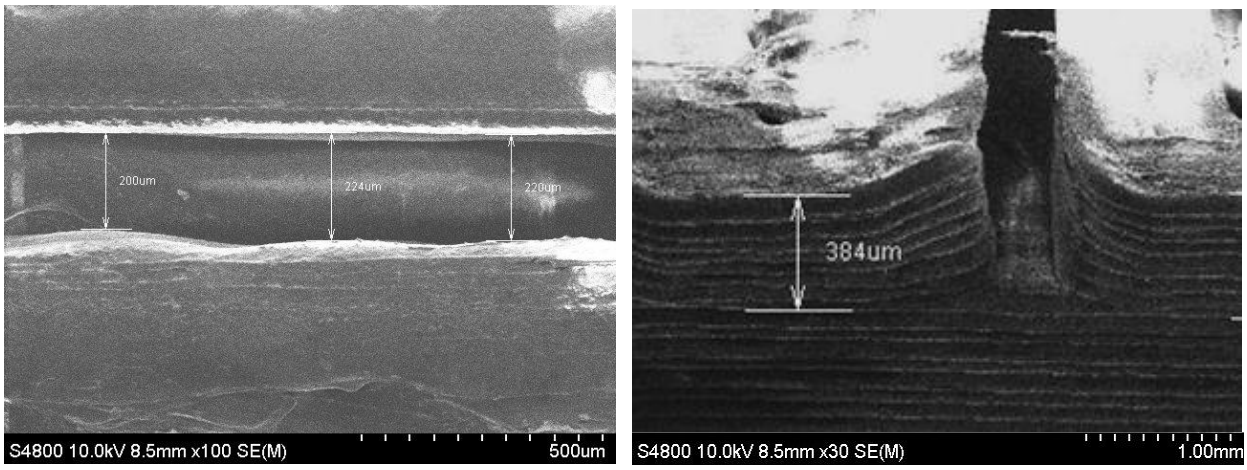

Figure 2. 3D printed microfluidic channels with a width of 220µm and height of 384µm.

A layer resolution of 100µm was used during the 3D printing process in order to ensure that the device had the high resolution required to produce the microchannel. As shown in **Figure 3** is the final fabrication laboratory on a chip device produced. The flat surface has been produced by printing the device face down onto the build platform. This has resulted is a flat polymer surface, which can be screen printed onto.

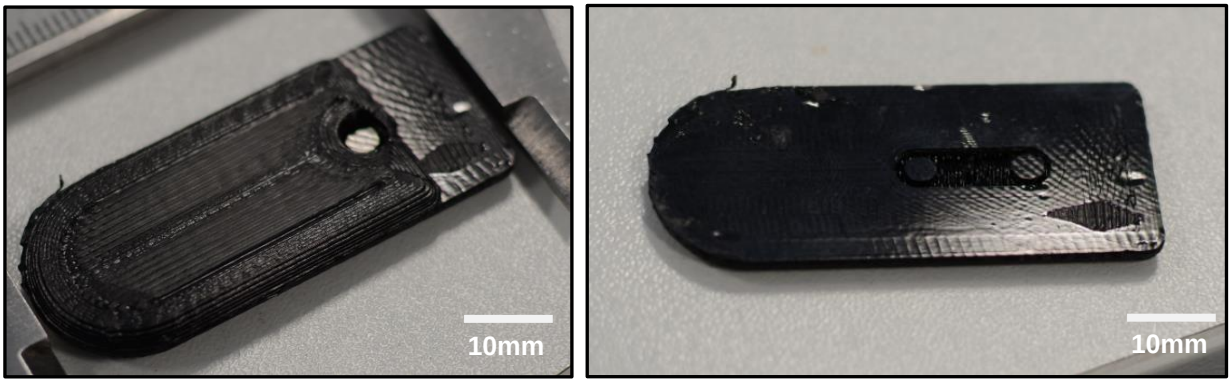

Figure 3. 3D Printed point of care device showing the internal microfluidic channels and chamber produced.

The 3D printed aliphatic polyurethane polymer used produced a microchannel was high hydrophilic and water tight. During the fabrication process, care has to be taken to ensure that the device is assembled concentrically and that the contacts are

aligned to the biosensor chip. The sides of the polymer device are then sealed with epoxy and a hydrophobic PDMS coating is added to the surface of the polymer. This is to ensure protection of the device before usage and that no fluid is able to make contact with the biosensing surface outside the area of the microchannel.

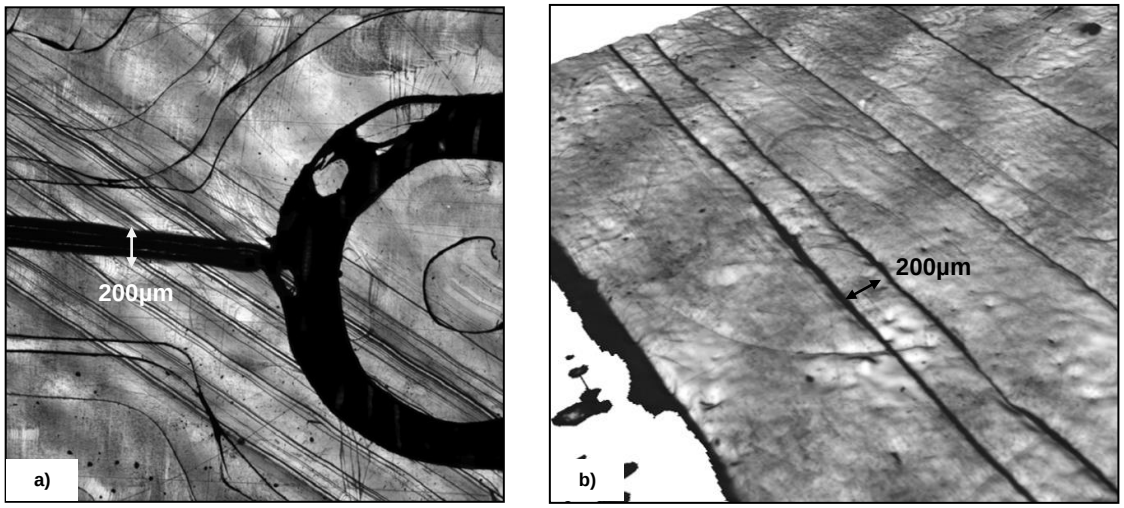

Figure 4. Micrographs of (a) the 3D printed microfluidic device architecture with and (b) 200µm width integrated microchannel.

As shown in **Figure 4a** is the curved aperture collector, which is used for receiving fluid to flow down the microchannel as shown in **Figure 4b** and over the exposed biosensor nanowires. By adjusting the depth of the microchannel, then this is used to control the thickness of a bio-fluid over the biosensor surface. Subsequently, a known quantity of fluid is used and then subsequently analyzed. **Figure 5** shows micrographs of the microchannels. The 3D printing process is capable of producing internal microchannel for a diameter of 200µm, below this, the microchannel became increasingly inconsistent.

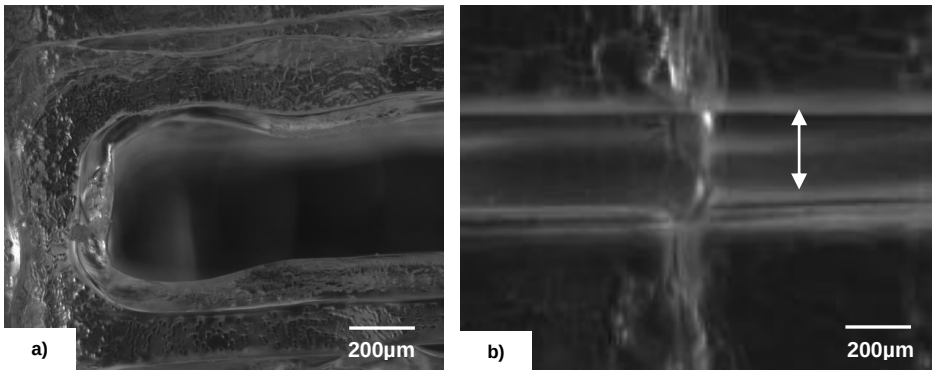

Figure 5. 3D printed microfluidic device with integrated (a) microchannel outlet and (b) cross section of the microchannel.

The polymer that was used to produce the microchannels was completely water tight and suffered no leakage as fluid passed along the microchannel. As shown in **Figure 6** liquid was placed into the inlet reservoir, the pressure of the gravity on the mass of

the liquid caused it to pass towards the restrictor. It is only when there is a volume of liquid pushing down is there a means of maintaining an active flow of liquid.

As fluid entered the microchannel from the reservoir as shown in **Figure 6a**. this process can only be achieved under an applied pressure. Under ambient pressure the liquid will move through the smaller microchannel. As a result, the liquid required pressure to be applied in order to produce a flow. This was achieved by ensuring that the reservoir was full. It is the weight of the liquid pushing down which induces a steady flow of liquid through the microchannel.

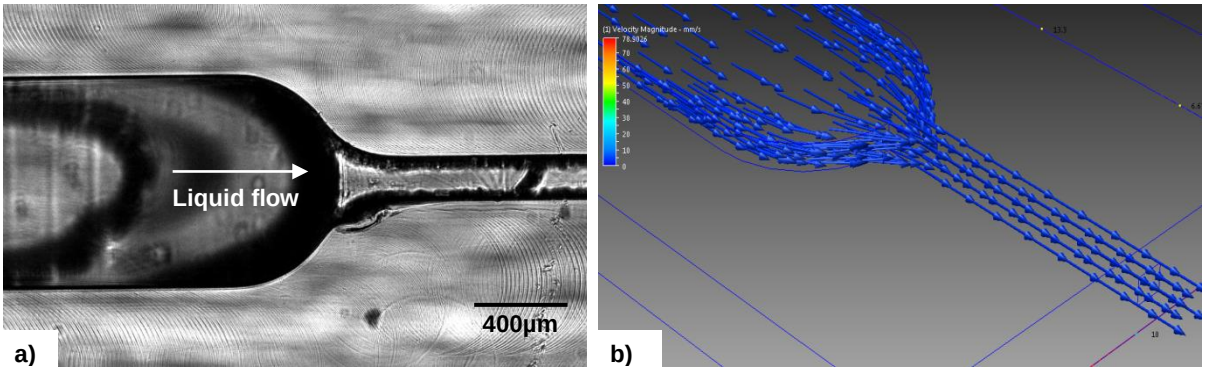

Figure 6. (a) Micrograph of the flow of fluid through a microchannel showing the movement of a fluid bead, and (b) Computational fluid dynamics of the fluid movement into a microchannel.

It is only when there is a larger volume of liquid pushing down through the microchannel is there a means of maintaining an active flow. As the computational fluid dynamics calculations show in **Figure 6b** as liquid is forced into the restrictor then there is an increase in its velocity. This microchannel configuration does offer one advantage over uniform length microchannels. Small volumes of liquid is passed through the microchannel, which can be sequentially analyzed by a biosensor.

3.3. Printed Electrical Contacts

Electrical properties of these contacts were measured to have a resistance of 45μΩ-cm. Silver ink was screen printed to produce electrical contacts as **Figure 7** shows. These are produced at a high level of geometrical accuracy, which minimizes variability in electrical measurements. This is critical for generating a reliable diagnosis.

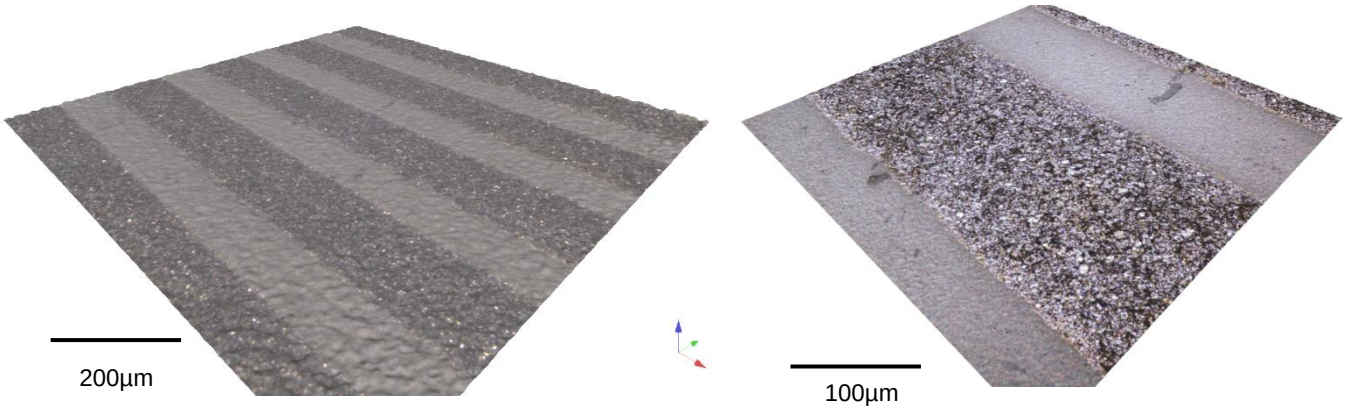

Figure 7. 3D surface profile micrographs of screen printed silver ink contacts.

Screen printed samples consistently print 200μm contact lines. White light interferometry (WLI) R_a values were measured at 3.04μm with an R_t value of 16.14μm. The profile of the printed indicates that there is both a low degree of variability produced by the screen printing process. This is important as these are required in-order to maintain a connection with the contacts of the biosensor.

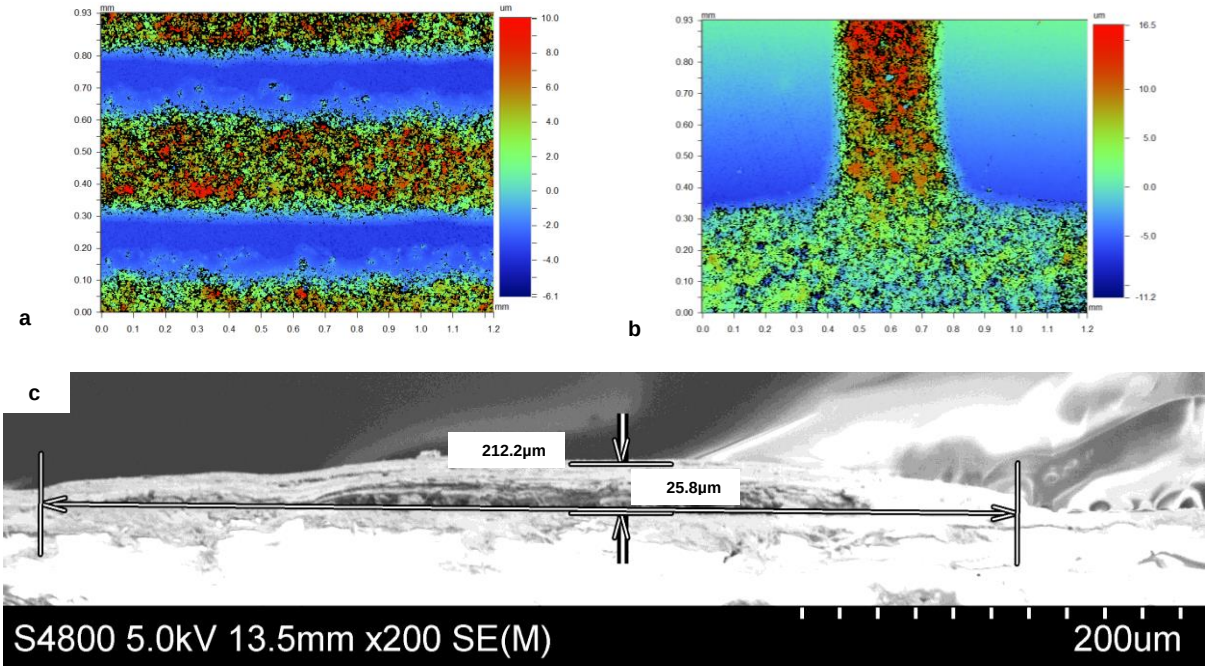

Figure 8. Profile of a 200μm wide screen printed silver contact deposited onto the surface of the 3D Printed APP substrate. (a) WLI measurement of a set of printed line contacts, (b) WLI measurement of a set of the region around a printed contact and (c) scanning electron micrograph of a cut section through the printed contact.

As shown in **Figure 8** is two WLI scans and SEM of the screen printed electrical contacts. These measured uniformly shaped printed structures would as a result have the required geometry to act as the biosensors electrical connections. As a result, this process allows for the combination in high throughput, accuracy and shape.

3.4. Printed Electronics and Biosensor Integration

This biosensor device is made in a four nanowire-based configuration as shown in **Figure 9** with a surface area of 25mm^2. Four SiNW lengths (50µm, 100µm, 300µm and 500µm) have been used during this work. The architecture of the device features the key components which make up a biosensor devices. There SiNW's generated during the fabrication process are 370nm in width. These are subsequently formed to 100µm width contact, which lead towards fourcontact pads at either side. These contact pads are subsequently connected to the screen printed contacts.

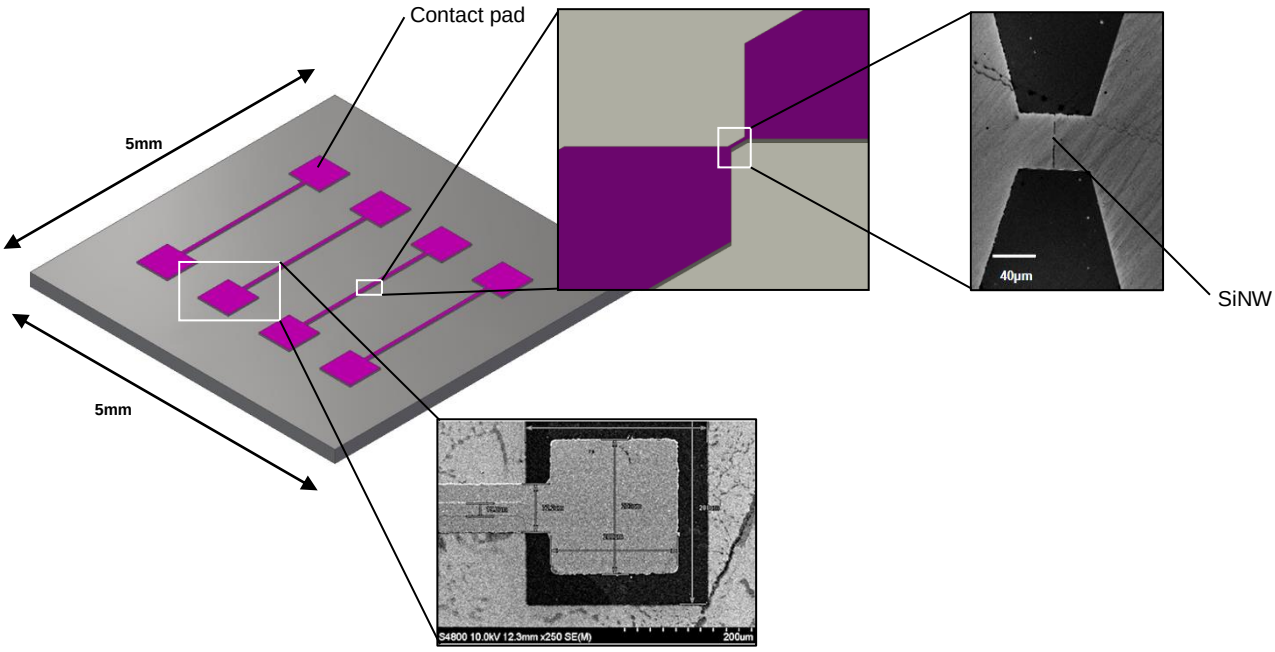

Figure 9. Architecture of the silicon nanowire-based biosensor chip, showing scanning electron micrographs of the silicon nanowire and the contact pads used to attach the silicon biochip to the screen printed contacts.

By measuring and comparing the electrical conductance of four nanowires simultaneously this allowed for the system to be electrically characterised accurately. Conductance testing is performed in order to ensure that a solid connection is made between the screen printed and biosensor. These measurements act to calibrate the electrical resistance of the device.

The resistances made directly from the SiNW Biochip and then through the flexographic printed contacts as **Figure 10** shows, suggest that although there is an offset between results these still follow the same general trend. Conductance testing

was performed on the sensor before and after it was applied to the microfluidic device. The resistance between the source and the contact points was measured both directly and through the flexoprinted contacts to determine the extra resistance due to the printing process.

The longer the nanowire then the more resistance it incurs. However, these results indicate that there is also non-uniformity in the thickness of each of the nanowires and this is why the results are not linear.

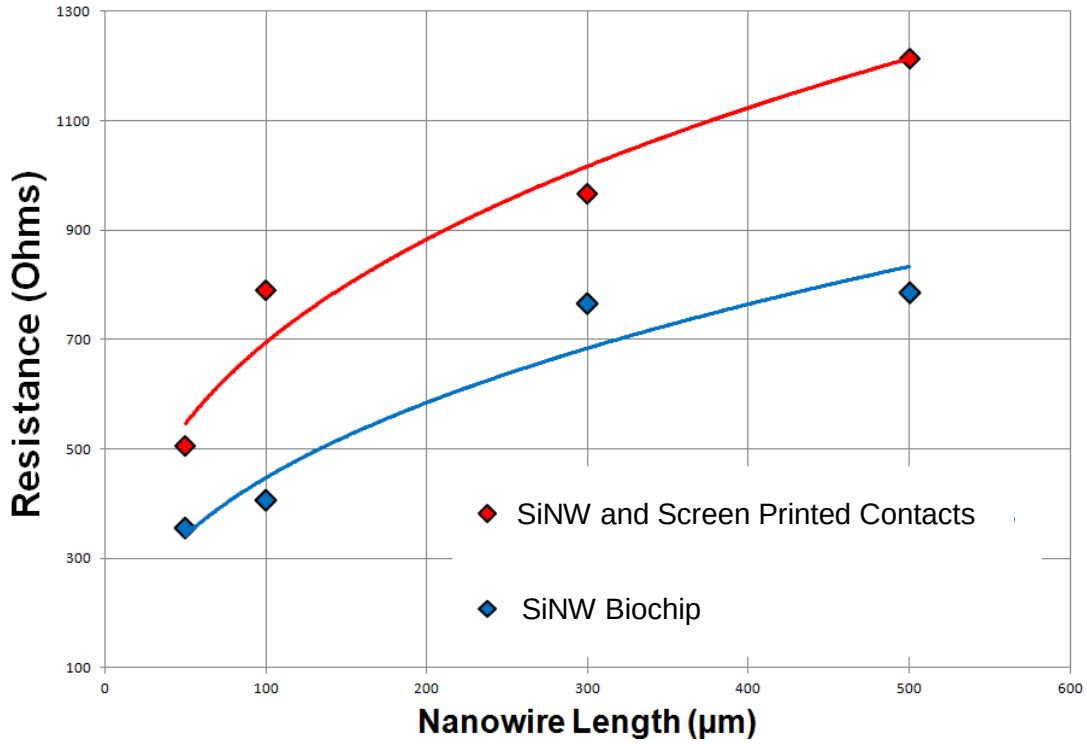

Figure 10. Comparison between nanowire length (µm) and resistance of the SiNW biochip.

The resistances made directly from the SiNW Biochip and then through the printed contacts as suggest that although there is an offset between results these still follow the same pattern. This suggests that the process developed during this result is valid for producing a nanowire-based point of care system.

4. Conclusions

One of the key problems which has prevented progress of lab-on-a-chip technology has been due to the manufacturing difficultly at the experimental level. The use of traditional methods of manufacture has resulted in problems in producing laboratory on a chip devices at a reasonable cost. 3D printing has allowed for the microfluidic element to be created flexibly, rapidly and with a wider variety of functionalities.

During this research an integrated 3D printed laboratory on a chip was developed, based on integrating conventional silicon biosensing systems with screen printed electronics. It was found that by integrating microchannel fabrication process using 3D printed polymers, this offered a means to towards the development of a microfluidic device. This research has also successfully developed the possibility of use of electrically integrating different elements through depositing screen-printed

silver contacts. This can lead to the development of point of care devices with many different elements having low resistance and high reliability. Creating this laboratory on a chip-based devices using 3D printing means they can be produced with a wide variety of materials of medical grade materials can be used. This represents the ability to manufacture nano-technological sensing devices and under controlled conditions.

References

[1] Zheng G, Lu W, Jin S, Lieber C.M. Synthesis and fabrication of high-performance n-type silicon nanowire transistors. Adv. Mater. 2004;16:1890-1893.
[2] Zheng G, Patolsky F, Cui Y, Wang W.U, Lieber C.M. Multiplexed electrical detection of cancer markers with nanowire sensor arrays. Nat Biotechnol. 2005;23:1294–1301.
[3] Patolsky F, Lieber C.M. Nanowire nanosensors. Materials Today. 2005;8:20-28.
[4] Patolsky F, Timko B.P, Yu G, Fang Y, Greytak A.B, Zheng G, Lieber C.M. Detection, stimulation, and inhibition of neuronal signals with high-density nanowire transistor arrays. Science. 2006;313:1100–1104.
[5] Patolsky F, Zheng G, Hayden O, Lakadamyali M, Zhuang X, Lieber C.M. Electrical detection of single viruses. Proc. Natl. Acad. Sci. USA. 2004;101:14017-14022.
[6] Patolsky F, Zheng G, Lieber C.M. Nanowire-based biosensors. Anal Chem. 2006;78:4260–4269.
[7] Patolsky F, Zheng G, Lieber C.M. Fabrication of silicon nanowire devices for ultrasensitive, label-free, real-time detection of biological and chemical species. Nat Protoc. 2006;1:1711–1724.
[8] Patolsky F, Timko B.P, Zheng G, Lieber C.M. Nanowire-based nanoelectric devices in the life sciences.MRS Bull. 2007;32:142–149.
[9] Patolsky F, Zheng G, Lieber C.M. Nanowire-based biosensors. Anal. Chem. 2006;78:4260-4269.
[10] Patolsky F, Zheng G, Lieber C.M. Nanowire sensors for medicine and the life sciences. Nanomedicine. 2006;1:51-65.
[11] Temiz Y, Kilchenmann S, Leblebici Y, Guiducci C. 3D Integration Technology for Lab-on-a-Chip Applications.Electronics Letters- IEEE. 2011;47:22-24.
[12] Temiz Y, Zervas M, Guiducci C, Leblebici Y. A CMOS Compatible Chip-to-Chip 3D Integration Platform. Electronic Components and Technology Conference (ECTC), San Diego, California, USA, May 29-June 2, 2012.
[13] Chard T. Pregnancy tests: a review. Hum. Reprod. 1992;7:701–710.
[14] Posthuma-Trumpie G.A, Korf J, van Amerongen A. Lateral flow (immuno)assay: its strengths, weaknesses, opportunities and threats. A literature survey. Anal. Bioanal. Chem. 2009;393:569–582.
[15] Clark T.J, McPherson P.H, Buechler K.F. The triage cardiac panel: Cardiac markers for the triage system. Point of Care.2002;1:42–46.

[16] Cosmi B, Palareti G, Moia M, Carpenedo M, Pengo V, Biasiolo A, Rampazzo P, Morstabilini G, Testa S. Accuracy of a portable prothrombin time monitor (Coagucheck) in patients on chronic oral anticoagulant therapy: a prospective multicenter study. Thromb. Res. 2000;100:279–286.
[17] Erickson K.A, Wilding P. Accuracy of a portable prothrombin time monitor in patients on chronic oral anticoagulant therapy: a prospective multicenter study. Clin. Chem. 1993;39,:283–287.
[18] Chen S, Selecman G, Lemieux B. Expanding Rapid Nucleic Acid Testing. IVD Technology. 2004;7:51-59.
[19] Jacobs E, Vadasdi E, Sarkozi L, Colman N. Analytical evaluation of i-STAT Portable Clinical Analyzer and use by nonlaboratory health-care professionals. Clin. Chem. 1993;39:1069–1074.
[20] Huh D, Gu W, Kamotani Y, Grotberg J.B, Takayama S. Microfluidics for flow cytometric analysis of cells and particles. Physiol. Meas.2005;26:73–98.
[21] Wu X.D, Chon C.H, Wang Y.N, Kang Y.J, Li D.Q. Simultaneous particle counting and detecting on a chip. Lab Chip, 2008;8:1943–1949.
[22] Yamada M, Seki M. Microfluidic particle sorter employing flow splitting and recombining. Anal. Chem. 2006;78:1357–1362.
[23] Woolley A.T, Hadley D, Landre P, de Mello A.J, Mathies R.A, Northrup M.A. Functional integration of PCR amplification and capillary electrophoresis in a microfabricated DNA analysis device. Anal. Chem. 1996;68:4081–4086.
[24] Sato K, Hibara A, Tokeshi M, Hisamoto H, Kitamori T. Integration of chemical and biochemical analysis systems into a glass microchip. Anal. Sci. 2003;19:15–22.
[25] Oh K.W, Ahn C.H. A review of microvalves. J. Micromech. Microeng. 2006;16:13–39.
[26] Sauer-Budge A.F, Mirer P, Chatterjee A, Klapperich C.M, Chargin D, Sharon A. Low cost and manufacturable complete microTAS for detecting bacteria. Lab Chip. 2009;9:2803–2810.

Nomenclature

Ar	Argon
APP	Aliphatic Polyurethane Polymer
FET	Field Effect Transistor
IPA	Isopropyl alcohol
MIBK	Methyl isobutyl ketone
MEMS	Microelectromechanical system
N_2	Nitrogen
NW	Nanowire
NW-FET	Nanowire Field Effect Transistor
POC	Point of Care
PDMS	Polydimethylsiloxane
PMMA	Polymethyl methacrylate
R_a	Arithmetic mean of departures from the mean line
R_t	Total height of profile
SiNW	Silicon Nanowire

SOI	Silicon on insulator
WLI	White Light Interferometry